

General Disclaimer

One or more of the Following Statements may affect this Document

- This document has been reproduced from the best copy furnished by the organizational source. It is being released in the interest of making available as much information as possible.
- This document may contain data, which exceeds the sheet parameters. It was furnished in this condition by the organizational source and is the best copy available.
- This document may contain tone-on-tone or color graphs, charts and/or pictures, which have been reproduced in black and white.
- This document is paginated as submitted by the original source.
- Portions of this document are not fully legible due to the historical nature of some of the material. However, it is the best reproduction available from the original submission.

COO-2059-4

A Facsimile Report

Reproduced by
UNITED STATES
ATOMIC ENERGY COMMISSION
Division of Technical Information
P.O. Box 62 Oak Ridge, Tennessee 37830



602 FACILITY FORM

ACCESSION NUMBER	14	(THRU)	G2
PAGE(S)	2	(CODE)	25
NASA CR OR TMX OR AD NUMBER		(CATEGORY)	
C21738		n71-001-043	



2059-4759 R

ABSTRACT

The Excitation of Ion
Bursts from Grids *

Georg Knorr

COO -3059-4

Department of Physics and Astronomy
The University of Iowa
Iowa City, Iowa 52240

April 1970

Experiments on ion bursts with a step function excitation of a grid are investigated theoretically. After the description of particle distributions and potentials in the sheath region, the ideal response of a probe located at a distance from the grid is calculated. It is shown how the declining part of the response function depends on the sheath characteristics. It is estimated that it should not be impossible to measure directly the far field of test particles in the initial part of the response function.

LEGAL NOTICE
This report was prepared as an account of work sponsored by the United States Government. Neither the United States nor the United States Atomic Energy Commission, nor any of their employees, nor any of their contractors, subcontractors, or their employees, nor any of their assigns, nor any individual, firm, or organization, nor any liability for the accuracy, completeness, or usefulness of any information, apparatus, product, or process disclosed, or represents, appears, would not infringe privately owned right.

* Research supported in part by the National Aeronautics and Space Administration under Contract NGR-001-043 and Atomic Energy Commission Grant No. AT(11-1)-2059.
Carl

I. INTRODUCTION

Experiments on pseudo waves or ion bursts have recently received considerable attention (ALEXEFF et al. (1968), LONGREN et al. (1967), TAYLOR and MACZENZIE (1968)). ALEXEFF et al. have observed simultaneously ion sound waves and pseudo waves when a grid was excited by sine wave trains. TAYLOR and MACZENZIE have excited pseudo waves by applying a voltage step function to a grid. This kind of excitation is perhaps the one most easily investigated theoretically.

Because ion bursts originate in the sheath region, information on the sheath might be obtained by studying ion bursts far away from the sheath. On the other hand, the ion burst traverses the plasma by which the burst is modified. So, also plasma properties could possibly be studied by means of pseudowaves. The investigation of these two possibilities is the purpose of this paper.

We consider a collisionless plasma only which is a good approximation to many experiments in question. At first, we have to study the sheath region which develops if a biased grid is immersed into a plasma. This can most easily be done by assuming firstly an ideal grid, i.e., a grid that does not draw current, irrespective of the voltage applied to it; and secondly, a step

voltage excitation. Due to the first assumption, the plasma displays no drift motion outside the sheath region and we may work with a Maxwellian plasma for both, ions and electrons. Due to the second assumption, the initial condition of the ion burst follows from the time independent Vlasov equation. If the voltage is suddenly removed from the grid, the particles in the sheath region have a certain velocity distribution, which is known. We can then solve the time dependent Vlasov equation and concentrate on those terms which represent the free streaming particles.

III. THE SHEATH

When a plane, negatively-biased grid of thin, crossed wires is immersed into a collisionless unmagnetized plasma, the ions are accelerated in the sheath region. Let the ion temperature be $\kappa T_i = \theta_i$ and the electron temperature be $\kappa T_e = \theta_e$. The steady state is then described by the time independent Vlasov equation for both particle species.

$$v \frac{df_{i,e}}{dx} + \frac{e}{m_{i,e}} \frac{\partial \varphi}{\partial x} \frac{\partial f_{i,e}}{\partial v} = 0 \quad (1)$$

The solution for the electrons, which are repelled from the sheath region is given by:

$$f_e = \frac{n_o}{\sqrt{2\pi\theta_e/m_e}} \exp[-(\frac{1}{2}mv^2 - e\varphi(x))/\theta_e] \quad (2)$$

and the density follows as $N_e(x) = n_o \exp[e\varphi(x)/\theta_e]$.

For the ions we obtain in a similar manner:

$$n_i(x) = \int f_i dv = \frac{2n_o}{\sqrt{2\pi\theta_i/m_i}} \int_{v_{min}}^{\infty} \exp[-(\frac{1}{2}m_i v^2 + e\varphi(x))/\theta_i] dv .$$

We have added a factor of two before the integral because we integrate over positive velocities only. The lower boundary of the integral, v_{min} is so far undetermined. If we put $v_{min} = 0$, we have thermodynamic equilibrium or, in other words, trapped ions in the sheath region. However, we have assumed our plasma to be collisionless, so the production rate of trapped particles due to collisions will be very low. Those particles which are trapped will oscillate rapidly in the sheath region. Eventually, even when the grid is almost ideal, the trapped ions will hit the wire and will be neutralized or absorbed. Thus, a steady state without trapped particles will rapidly develop and we have to choose

$$v_{min} = (-2e\varphi_0/m_i)^{1/2} .$$

The ion density can then be written as:

$$n_i = \frac{\partial}{\partial(\epsilon\varphi)} \left\{ -\frac{2n_o}{\sqrt{\pi\theta_i}} \int_{-\sqrt{\epsilon\varphi}}^{\infty} \exp(-v^2/\theta_i) dv \right\} . \quad (3)$$

If we insert the results (1) and (2) into Poisson's equation, we obtain:

$$\frac{d^2}{dx^2} e\varphi = -k\pi e^2 n_0 \frac{\partial}{\partial e\varphi} \psi, \quad (4)$$

where

$$\psi(e\varphi) = -2/\sqrt{\pi\theta_1} \int_{-\infty}^x \sqrt{\epsilon - e\varphi(x)} \exp(-\epsilon/\theta_1) d\epsilon - \theta_e \exp(e\varphi/\theta_e) + C.$$

It is easily seen that $\psi(e\varphi)$ is a convex function of $e\varphi$. From the well known analogy of Eq. (4) with the equation of motion of a particle in a potential well, we can immediately conclude that the spacial dependence of the potential in the sheath must be a monotone decreasing function of the distance from the grid. Equation (4) can be integrated. Taking into account that $d\psi/dx = 0$ when $\varphi = 0$, we obtain

$$\frac{d}{dx} [\exp(x)] = [8\pi e n_0 (-\psi(e\varphi(x)) - (\theta_1 + \theta_e))]^{1/2} \quad (5)$$

Some limiting cases are of interest now: We consider first the case $-e\varphi/\theta_1 \ll 1$. This condition applies to the outer rim of the sheath, where most of the potential has already been screened out. It describes the transition to the unperturbed plasma.

Integrating Eq. (5) gives

$$-e\varphi(x)/\theta_1 = [(-e\varphi_0/\theta_1)^{1/4} - 0.307 x/\lambda_d]^4 \quad (6)$$

where φ is the potential applied to the grid. The remarkable feature is that φ vanishes at a finite distance, contrary to the familiar exponential result.

If only a small potential is applied to the grid, satisfying above inequality, the dimension of the sheath is given by

$$L = \lambda_{Di} 3.27 (-e\varphi_0/\theta_1)^{1/4} \quad (7)$$

where $\lambda_{Di} = (\theta_1/M_w \rho_i)^{1/2}$ is the ion Debye length.

The experimentally interesting case is characterized by the inequality

$$(-e\varphi/\theta_1)^{1/2} \gg 1 \quad (8)$$

In this limit, we obtain the asymptotic formula

$$-e\varphi(x)/\theta_1 = \left[(-e\varphi_0/\theta_1)^{3/4} - \frac{3}{2\pi^{1/4}} \frac{x}{\lambda_{Di}} \right]^{1/3} \quad (9)$$

The dimension of the sheath is consequently given by

$$L = 0.84 \lambda_{Di} (-e\varphi/\theta_1)^{3/4}. \quad (10)$$

This is Langmuir's sheath formula (See CHEN (1965)). Eq. (9) becomes invalid when x is close to L , because then inequality (8) is no longer

satisfied. However, this affects only a very small part of the sheath, such that Eq. (10) is a valid expression.

Let us assume as typical values for an ion burst experiment: electron temperature 1 eV, ion temperature 1/20 eV, applied potential $\epsilon_{\text{ap}} = 100 \text{ eV}$, ion species: Xenon (atomic mass 131), density: $n_0 = 10^8 \text{ cm}^{-3}$.

With these values, one obtains for the electron Debye length $\lambda_{\text{De}} = 0.07 \text{ cm}$ and the sheath dimension $L = 0.42 \text{ cm} = 61.5 \lambda_{\text{De}}$. It follows that the grid may be quite coarse, and yet have good screening properties.

With above data, we obtain the following values, which we list for future reference: Number of particles in a Debye sphere $N = k\eta/3 n \lambda_D^3 = 1.43 \times 10^5$, thermal velocity of electrons $v_e = 6 \times 10^7 \text{ cm/sec}$. Velocity of accelerated ions: $V = 1.38 \times 10^5 \text{ cm/sec}$. The electron self-collision time turns out to be: $t_c = 1.9 \times 10^{-4} \text{ sec}$ (SPITZER (1956)). The electron plasma can still be regarded as collisionless. For any numerical estimate, we will refer to this set of parameters.

III. THE ION BURST

Let us assume as typical values for an ion burst experiment: electron temperature 1 eV, ion temperature 1/20 eV, applied potential $\epsilon_{\text{ap}} = 100 \text{ eV}$, ion species: Xenon (atomic mass 131), density: $n_0 = 10^8 \text{ cm}^{-3}$.

When the bias of the grid is removed at $t = 0$, the perturbed distribution function in the sheath region may be taken as the initial value for a solution of the Vlasov equation. Confining ourselves to a linear solution, we neglect some nonlinear effects close to the sheath region, because the disturbed distribution is not small compared to the background distribution. But, as the ions travel along, they spread in phase space, because they have different initial velocities in different locations in the sheath. Their density decreases and eventually the linear theory becomes applicable.

Experimentally this means that we have to observe the ion burst at some distance from the grid.

We may immediately write down the well known result of the linear theory (see MONTGOMERY and TIDMAN (1962))

$$-\nabla q_k = E_k = \hat{k} \cdot \frac{i\omega_{\text{ren}}}{ik} \frac{f_k^{(1)}(t=0) - f_k^{(e)}(t=0)}{p + ik \cdot \underline{v}} \hat{k}^2 \quad (11)$$

where \hat{k} is the unit vector of k . $E_k(p)$ is the Fourier transform in space and Laplace transform in time of the electric field $E(z, t)$:

$$\underline{E}(\underline{x}, t) = -\nabla \phi(\underline{x}, t) = \int_{-\infty}^{+\infty} \frac{d^3 k}{(2\pi)^3} \exp(i\underline{k} \cdot \underline{x}) \int_{-\infty}^{+\infty} \frac{dt}{2\pi i} \exp(pt) \underline{E}_k(p). \quad (12)$$

The plasma dispersion function is given by

$$D(\underline{k}, p) = 1 + \frac{u_e^2}{ik} \int \frac{\underline{k} \cdot \partial F^i / \partial v}{p + ik \cdot \underline{v}} d^3 v + \frac{p_e}{ik} \int \frac{\underline{k} \cdot \partial v_o^i / \partial v}{p + ik \cdot \underline{v}} d^3 v \quad (13)$$

where F_o^i are the normalized homogeneous distribution functions for ions and electrons, respectively. Evaluation of the integrals gives the desired potential distribution around the group of ions traversing the plasma.

It is convenient to write

$$f_1^i(\underline{x}, \underline{y}, t=0) = g(\underline{x}, \underline{y}) = \int d^3 \underline{z} \int d^3 \underline{v} \delta(\underline{x} - \underline{z}) \delta(\underline{v} - \underline{y}) \quad (14)$$

and to compute $\phi(\underline{x}, t)$ for

$$f_1^i(t) = \delta(\underline{x} - \underline{z}) \delta(\underline{v} - \underline{y}) \quad (15)$$

only. This is the Green's function of the problem, and the actual solution is obtained from it by an integration.

We assume that the velocity of the ions v_i in the sheath is much larger than the phase velocity v_p of the ion acoustic wave. This

is the case in many experiments and serves to keep the two phenomena spatially separated. With the initial distribution Eq. (15), the potential in Eq. (11) can be written as

$$\phi^T(\underline{x}, t; \underline{z}, \underline{y}) = 4\pi n_o \int \frac{d^3 k}{k^2 (2\pi)^3} \exp[-ik \cdot (\underline{x} - \underline{z} - \underline{v}_o t)] D(\underline{k}, -ik \cdot \underline{v}_o)^{-1}. \quad (16)$$

In Eq. (16) we have omitted contributions from the inverse Laplace transform resulting from zeros of $D(\underline{k}, p)$ which represent various ion acoustic and plasma waves, which are of no interest to us. Eq. (16) is the potential of a test particle starting from $\underline{x} = \underline{z}$ with velocity \underline{v}_o at $t = 0$ (compare THOMPSON (1962)). We defer an evaluation of the integrals of Eq. (16) until later and anticipate only, that the test particle potential can be written as

$$\phi^T(\underline{x}, t; \underline{z}, \underline{y}) = \exp(-k_o r)/r + \chi(\underline{x}, t; \underline{z}, \underline{y}). \quad (17)$$

\underline{x} is the position of the particle at time t , \underline{z} and \underline{y} are the initial position and velocity at time zero, $r = |\underline{x} - \underline{z} - \underline{y}|$ is the distance from the test particle at time t . The first term on the right side of Eq. (17) represents die Debye screening and χ contains all the rest. χ vanishes if the test charge is at rest. Because the first term is symmetric, all particle-particle and wave-wave interactions

are contained in the second term. COOPER (1969) has recently calculated the second term in Eq. (17) for the case of a slow test charge in an electron plasma.

When an ideal probe is inserted a distance x_0 from the grid (compare Fig. 1) it should pick up a voltage signal very similar to the signal in Fig. 2b of ALEXEFF et al. (1968). The schematic form of the resulting voltage trace is shown in Fig. 2 by the line $a-c-e$.

When the probe is replaced by an ideal particle detector, we should observe a similar curve, however, commencing later in time and then rising faster than the voltage response function. We expect a line above. The difference between $a-c$ and $a-b$ represents the potential which forms ahead of the ion burst. It is a superposition of the long range test particles potentials contained in the x term of Eq. (17).

We consider now the superposition of the test particle potential, by integrating over all particles:

$$\phi(x, t) = q \int d\xi [d\epsilon(\xi)] \phi^*(x, t; \xi)]$$

Note that $\epsilon(\xi)$, the distribution function of accelerated ions for $t=0$, vanishes everywhere, except in the sheath. Neglecting the small thermal spread (the ions are usually quite cool) we can write: $\epsilon(\xi) = n_1(\xi) + (v_m(\xi)-1)$. The ion density $n_1(\xi)$ is given by:

$$n_1(\xi) = n_0(2\theta_1/\pi M)^{1/2} / v_m(\xi)$$

It has been assumed that $qV_0 \gg \frac{1}{2} M(v_i^{th})^2$, where V_0 is the applied grid potential and v_i^{th} the thermal ion velocity.

Taking into account only the first term on the right hand side of Eq. (17), which represents the Debye screening, we obtain:

$$\begin{aligned} \phi(x, t) = q \int d\xi [d\eta] n_1(\xi) & \delta(v_m(\xi)-1) \exp[-k_d |x - \xi - \eta|] \\ & \cdot [x - \xi - \eta]^{\alpha-1}. \end{aligned}$$

The integration over η can immediately be carried out to give:

$$\phi(x, t) = q \int d\xi n_1(\xi) \exp[-k_d |x - \xi - t v_m(\xi)|] \cdot |x - \xi - t v_m(\xi)|^{-1}.$$

This integral can be evaluated if we consider that

$$\lim_{k_d \rightarrow \infty} k_d^2 \exp(-k_d r) / r \pi r = \delta(r)$$

k_d is not infinite in our case, but of the order of 15 cm^{-1} . This is much larger than the typical inverse length which characterizes $n_1(\xi)$, so that the approximation is justified. We thus obtain

$$\varphi(x_o, t) = q(2/n)^{1/2} n_o (\theta_1/M)^{1/2} (v_m(\xi))^{-1} k_d^{-2} \left| \frac{dv_m(\xi)}{d\xi} \right|^{-1} \quad (18)$$

ξ has to be taken such that $x_o = \xi + tv_m(\xi)$. This simply means that the particles which arrive at the probe located at x_o after time t started at $t = 0$ from location ξ with velocity $v_m(\xi)$. A glance at Fig. 1 indicates that in general, two different values ξ satisfy the condition, characterizing particles originating immediately before and behind the grid. It can easily be arranged experimentally that

$$\frac{dv_m(\xi)}{d\xi} \gg 1,$$

so that the one in the denominator of Eq. (18) can be neglected. We also have conservation of energy in the sheath region: $qV(\xi) + \frac{1}{2} M V_m(\xi)^2 \approx 0$. Differentiating this relation, we can finally rewrite Eq. (18) as

$$\varphi(x, t) = (\theta_1/n M)^{1/2} n_o k_d^{-2} t \left| \frac{1}{E(\xi)} \right| x_o = \xi + tv_m(\xi) \quad (19)$$

ξ has again to be chosen so that $x_o = \xi + tv_m(\xi)$. $E(\xi)$ is the electric field for $t = 0$ in the sheath at ξ .

We see that the particle contributes to the potential at x_o , is inversely proportional to the electric field E , which it experienced

at $t = 0$. The singularity for $E \rightarrow 0$ is only an apparent one because we have assumed large electric fields in deriving Eq. (19). So

Eq. (19) holds only for the initial part of the response curve in Fig. 2, and this is all we are interested in. The damping with t^{-1} is a purely kinematic effect.

In order to obtain the voltage response of a probe as a function of time from Eq. (19), we observe that the potential in the sheath can be described as $V = V_o (1 - \xi/L)^\nu$, at least for small ξ . For $\nu = 4/3$, we recover the Langmuir sheath potential. In this case, the sheath thickness is given by Eq. (10). Using the conservation of energy, we can write for the ion velocity in the sheath:

$$v_m(\xi) = x_o/t = (-2qV_o/M) (1 - \xi/L)^{\nu/2}.$$

x_o is the distance from grid to probe.

Expressing the potential at x_o in terms of x_o and t , we find:

$$\varphi(x_o, t) = (2n\theta_1/M)^{1/2} (-2qV_o/M)^{-1+1/\nu} \frac{n_o L}{k^2 V_o x_o^{2-\nu}} \frac{t^{1-2/\nu}}{2},$$

for $t > x_o/(v_m \max)$

$$\varphi(x_o, t) = 0; \text{ for } t < x_o/(v_m \max) \quad (20)$$

For the case of a Langmuir potential, $v = 4/3$ and we obtain

$$\varphi(t) \sim t^{-1/2} \quad (21)$$

We recall that in computing Eq. (20) we have replaced the Debye screening factor by a delta function. Thus, φ in Eq. (20) is actually proportional to the charge distribution as it passes by the tip of the probe.

Equation (21) describes the decay of the signal as displayed in Fig. 2b of LÖNNQVIST et al. (1967). As we have omitted any additional damping like Landau and collisional damping, the influence of non-ideal geometry, the observed damping should be somewhat faster than $t^{-1/2}$. The response function Eq. (20), which is drawn in Fig. 2 by the line above has an infinite slope at b. This is due to the substitution of the delta function for the Debye screening term. If one did the calculation correctly, the spatial potential should rise not infinitely steep but over a Debye length or two. This corresponds to a blurring of the curve in Fig. 2 in the region b-c by an amount $\Delta t = \lambda_d / v_{ion}$. With $\lambda_d = 7 \cdot 10^{-1}$ cm and $v_{ion} = 7 \cdot 10^5$ cm/sec, we find $\Delta t = 10^{-1}$ μ sec. An inspection of Fig. 2b of ALEXEFF et al. (1968) shows that the rise time from zero to the maximum is definitely longer, namely about $8 \cdot 10^{-1}$ μ sec. Although the experimental conditions do not quite correspond to the case treated here, it may

be speculated that the slower rise time is due to that part of the test particle potential which is not due to the Debye screening. Or in other words, it may be due to the expression x in Eq. (17), which we study now in more detail.

IV. THE FAR FIELD TEST PARTICLE POTENTIAL

The evaluation of the integrals constituting the test particle potential (16) in the general case is quite involved, even if only an electron distribution is considered. MONTGOMERY et al. (1968) have shown for an electron plasma that for a moving test particle, the far field is not exponentially decreasing as in Debye screening, but rather exhibits a quadrupole field in lowest significant order. Recently, COOPER (1969) derived an expression for the quadrupole field if the test particle velocity is small compared to the thermal electron velocity. This condition is also satisfied in ion burst experiments. We should, however, also take into account the ion distribution function. This complicates the mathematics because an additional resonance in $D(k, p)$ appears, corresponding to the excitation of ion waves. But because of the large ion mass, this effect should be quite small and we neglect it.

COOPER'S formula for the far field reads

$$\begin{aligned} x(x, t; \xi, \eta) = & 2q/\sqrt{\epsilon_0 k_D^2} (\nabla r)^2 [\sqrt{2\pi} \cos \theta + \sqrt{\epsilon_0/m} (1 - \frac{\eta}{2}) \\ & (1 - 3 \cos^2 \theta)] \end{aligned}$$

where $\cos \theta = \hat{z} \cdot \hat{r}$. The geometry which we want to consider is shown in Fig. 3. A particle cloud having a density n_0 is moving through

the plasma filling a disk between r_{\min} and r_{\max} from the probe. The potential due to the quadrupole fields is obtained by integrating over the cloud which results in

$$\varphi_{\text{probe}} = (2\pi/k_d)^2 (\sqrt{\epsilon_0/m} \int_{r_{\min}}^{r_{\max}} \frac{\rho(x)}{x} dx) \quad (23)$$

When $|r_{\max} - r_{\min}|/r_{\min} < 1$, this is of order of magnitude

$$\varphi_{\text{probe}} \sim 2\pi \lambda_o^2 \sqrt{\epsilon_0/m} \Delta r/r_{\min}, \quad (24)$$

where $\Delta r = r_{\max} - r_{\min}$. To estimate the order of magnitude of the potential (24), we compare it with the potential which is seen by an ideal probe when immersed into a Debye screened charge distribution with constant charge density ρ_0 .

Such a probe sees a potential

$$\varphi = \int \rho_0 \exp(-r/\lambda_o)/r dr = \varphi \pi \lambda_o^2 \rho_0. \quad (25)$$

When $\Delta r/r$ is of order one the far field potential is smaller by a factor $\sqrt{\epsilon_0/m}$ which however, may be fairly large, 1/10 to 1/5 say. Thus, it is not completely out of question, that the test particle potential can be measured. A disadvantage is that probes are usually

biased to increase their sensitivity which depletes the plasma of electrons and which may be detrimental to the observation of the test particle potentials.

So far, we have assumed that the test particles move with a constant velocity. The ions see, however, an electric field which is due to the dragging electron cloud and which tends to slow them down. We estimate the order of magnitude of this effect.

The force on a test particle is given by the "frictional force":

$$\mathbf{F} = \frac{q^2}{\lambda_d^2} \frac{\eta}{2\sqrt{\theta_e/m}} \ln \Lambda \quad (26)$$

Λ is of the order of the inverse plasma parameter. The force (26) acts on a particle during the time $t = x_0/\eta$ and the displacement Δx from its unperturbed path of flight at time t is

$$\Delta x = \frac{1}{2} \frac{F t^2}{M} = \left(\frac{1}{16\pi N} \frac{\eta}{M} \ln \Lambda \right) \frac{x_0^2 w_{pe}^2}{\sqrt{\theta_e/m}} \lambda_d$$

Using the experimental values quoted earlier this amounts to $\Delta x \sim 10^{-4} \lambda_d$. This shows that the effect is completely negligible.

V. CONCLUSIONS AND EXPERIMENTAL CONSIDERATIONS

When a group of fast ions originating from a grid traverses in a plasma and sweeps by an ideal probe, the potential recorded has the form as depicted in Fig. 2. The latter part, cde, of the potential trace is determined by the form of the potential around the grid. For a Langmuir sheath, it decays like $\varphi \sim t^{-1/2}$.

The onset a-c of the potential may be influenced by the far field part of the test particle potential of the fast ions, which precedes the ions by 10 and more Debye lengths. An estimate shows that it might be observable. The following features could improve the experimental investigations beyond existing experiments: The grid should be excited by a step function such that the grid is biased negatively for $t < 0$ and on floating potential for $t > 0$. The step function seems to be most easily amenable to a theoretical analysis.

In practice, it is not possible to change the bias of a grid instantaneously. The ions in the sheath region do not keep the velocity they had at $t=0$, but are decelerated to some extent. This can be taken into account by considering an effective velocity distribution of the ions at $t = 0$. This effective distribution and an infinitely fast potential change is equivalent to the real

distribution and a potential change in finite time. The main difference of the two distributions is that the peak of the effective distribution is at a lower potential.

When the applied grid voltage is large (typically 50 - 100 Volts) the plasma might be affected by it and might be driven unstable. This can be avoided by using a triple grid. The two outer grids are kept at floating potential, whereas, the middle grid is biased. The plasma is then shielded from the large potential. In addition, a triple grid keeps the area where the ions are accelerated much smaller than a single grid. The mesh size of the outer grids should be smaller than the Debye length, which is of the order of a millimeter.

Simultaneously, with the ion burst, an ion acoustic wave signal is launched. Both signals should be well separated at the location of the probe in order to analyze them separately. This is accomplished by making the particle velocity much larger than the phase velocity and keeping a long distance between grid and probe.

A voltage detector and a particle detector should be used in the same experiment. We expect that the voltage detector will measure a curve similar to acde in FIG. 2, whereas, the particle detector will measure a curve similar to acde. A suitable particle detector has recently been described by IKEZI and TAYLOR (1969). Such an experiment should yield valuable information on the effective range of the far field as well as on the nature of the sheath under different conditions.

ACKNOWLEDGEMENTS

The author wishes to thank Dr. I. Alexeff for a very thorough discussion. Other stimulating discussions with Professors K. Lonngren, D. Montgomery, and D. Gurnett, as well as with Dr. F. Sluijter are also gratefully acknowledged. I am grateful to Dr. S. Aksornkitti for making accessible to me unpublished experimental material. This work was supported in part by National Aeronautics and Space Administration Grant NGR-16-001-013 and Atomic Energy Commission Grant No. AT(11-1)-2059.

REFERENCES

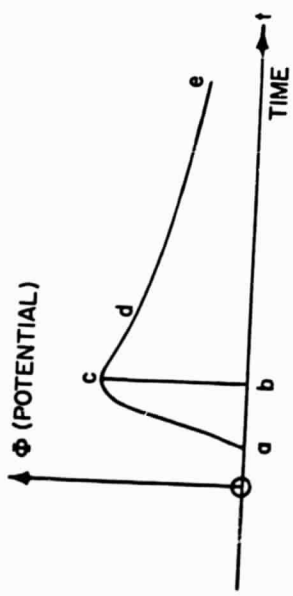
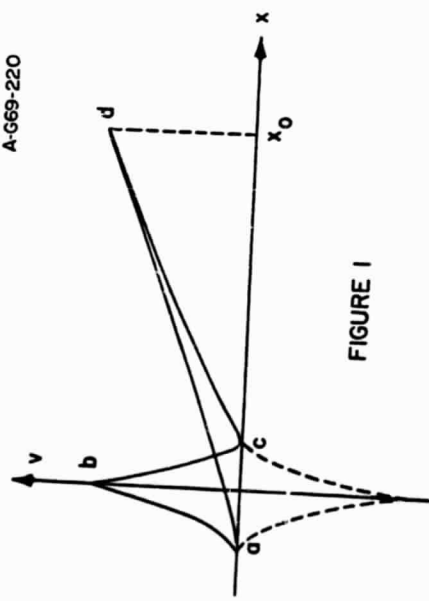
- ALEXEFF, I., JONES, W. D., LONNGREN, K. (1968) *Phys. Rev. Letters* 21, 878.
- CHEI, P. (1965) in *Plasma Diagnostic Techniques*, HUDDLESTONE, R. H. and LEONARD, S. I., eds. Academic Press.
- COOPER, G. (1959) *Phys. Fluids* 2, 2707.
- IKEZI, H. and TAYLOR, R. F., Report 12-42, Plasma Physics Group Department of Physics, UCLA, February, 1969.
- LONNGREN, K., MONTGOMERY, D., ALEXEFF, I. and JONES, W. D. (1967) *Physics Letters* 25A, 629.
- MONTGOMERY, D. C. and TIDMAN, D. A. (1962) *Plasma Kinetic Theory*, McGraw-Hill, Chapter 5.
- MONTGOMERY, D. C., JOYCE, G., and SUGIHARA, R. (1968) *Plasma Physics* 10, 681.
- SPITZER (1956) *Physics of Fully Ionized Gases*, Interscience Publishers, Inc., New York, p. 78.
- TAYLOR, R. F. and MCKENZIE, K. R. (1968) Bulletin APS 13, 1498 and Report Plasma Physics Group, Department of Physics, UCLA, November, 1968.
- THOMPSON, W. B. (1962) *An Introduction to Plasma Physics*, Pergamon Press, Chapter 8.

FIGURE CAPTIONS

- Figure 1. Schematic indication of the location of accelerated ions in phase space. For $t = 0$, ions are located along the line abc, within the sheath region; for $t > 0$ they travel along straight line trajectories and are found along adc, for instance. The dotted line represents particles, which go to the left.
- Figure 2. Schematic plot of a typical probe potential, as the ions burst sweeps by the probe tip. The part bcd is due to the space charge of the particles. The long range test particle potential forms ahead of the ions, corresponding to the part ec of the curve.
- Figure 3. Schematic plot of a cloud of ions tip-sweeping a probe. The ions are located between r_{\max} and r_{\min} . The quadrupole part of the test particle potential reaches beyond the ion cloud.

27

A-669-220



28

A-G70-178

